Available online at www.sciencedirect.com
ScienceDirect
Journal of Solid State Chemistry 180 (2007) 127–131
JOURNAL OF SOLID STATE CHEMISTRY
www.elsevier.com/locate/jssc

Green and red upconversion luminescence in $CeO_2:Er^{3+}$ powders produced by 785 nm laser

Hai Guo[a,b,*]

[a]Department of Physics, Zhejiang Normal University, Jinhua, Zhejiang 321004, PR China
[b]Zhejiang Key Laboratory for Reactive Chemistry on Solid Surfaces, Institute of Physical Chemistry, Zhejiang Normal University, Jinhua 321004, PR China

Received 22 August 2006; received in revised form 24 September 2006; accepted 1 October 2006
Available online 10 October 2006

Abstract

$CeO_2:Er^{3+}$ powders were prepared by Pechini type sol–gel method. The structural properties of $CeO_2:Er^{3+}$ were studied by X-ray diffraction (XRD) and Fourier transform infrared (FT-IR) spectra. The results show that $CeO_2:Er^{3+}$ has low phonon cutoff energy, which indicate that $CeO_2:Er^{3+}$ may have high luminescent efficiency. The green and red upconverted luminescence spectra of Er^{3+} were investigated under excitation into the $^4I_{9/2}$ level by 785 nm laser. The upconversion mechanisms were studied in detail through laser power dependence and Er^{3+} ions concentration dependence of upconverted emissions, and results show that excited state absorption and energy transfer process are the possible mechanisms for the upconversion. The upconversion properties indicate that $CeO_2:Er^{3+}$ may be used in upconversion phosphors.

PACS: 78.55 −m

Keywords: $CeO_2:Er^{3+}$; Upconversion; Excited state absorption; Energy transfer process

1. Introduction

In the past few decades, the upconversion luminescence of infrared light to visible light of different materials, such as single crystals, optical fibers, nano-materials, ultrafine powders and glasses, has been investigated extensively, due to the search for all-solid compact laser devices operating in the violet–blue–green region, upconversion phosphors, infrared quantum counter detectors, fluorescent labels for sensitive detection of biomolecules, temperature sensors and three-dimensional displays [1–21]. More recently, the availability of high-power infrared laser diodes has stimulated researches in the areas of upconversion [8,21].

In upconversion process, two (or more) low-energy photons from excitation source are converted into one photon with higher energy. Trivalent rare earth ions such as Er^{3+}, Tm^{3+}, Ho^{3+} and Yb^{3+} are doped as absorption and (or) emission centers in upconversion materials [3,6,11,14]. Among these rare earth ions, the Er^{3+} ion is the most popular as well as one of the most efficient ions for upconversion because the metastable levels $^4I_{9/2}$ (around 12,491 cm^{-1}) and $^4I_{11/2}$ (around 10,276 cm^{-1}) of Er^{3+} can be conveniently populated by commercial low-cost high-power 800 and 980 nm laser diodes, respectively [8,10,11].

The upconversion performance of a material could be enhanced significantly by suitable selection of host matrix [5,11,13]. Numerous oxide host matrixes, such as Y_2O_3 [4,6–8], Gd_2O_3 [9,11,12], ZrO_2 [13,14], TiO_2 [15], $BaTiO_3$ [15] and $SrTiO_3$ [16], have been investigated as host matrix for upconversion phosphors due to their low vibrational frequencies.

Cerium oxide (CeO_2) is a well-known functional material used in many fields. It is a promising host material for upconversion because of its good thermal stability and low phonon cutoff energy (465 cm^{-1}) [22–24]. The former property makes it suitable for practical application, and the later one would decrease the possibility of nonradiative

*Department of Physics, Zhejiang Normal University, Jinhua, Zhejiang, 321004, PR China.
E-mail address: ghh@zjnu.cn.

0022-4596/$ - see front matter © 2006 Elsevier Inc. All rights reserved.
doi:10.1016/j.jssc.2006.10.003

transitions and in turn result in a high quantum yield of upconverion process. In addition, CeO_2 can be easily doped with rare earth ions, which means high concentration doping is possible. But to the best of my knowledge, there is no report on upconversion properties of CeO_2:Er^{3+} powders.

In this paper, CeO_2:Er^{3+} powders were prepared by Pechini type sol–gel method. The structural properties of samples were characterized by XRD and Fourier transform infrared (FT-IR) spectra. Under excitation into $^4I_{9/2}$ level by 785 nm laser, strong green and red upconversion emission of CeO_2:Er^{3+} were recorded. The upconversion mechanisms were studied in detail through laser power dependence and Er^{3+} ions concentration dependence of upconverted emissions. Excited state absorption (ESA) and energy transfer (ET) process are discussed as possible mechanisms for the upconversion.

2. Experimental

Sol–gel method is suitable to prepare optical materials as it permits the mixing at molecular level and low processing temperature [17]. In this paper, CeO_2:Er^{3+} powders with different doping concentration (0.5%, 1%, 3% and 6% (molar fraction)) were prepared by Pechini type sol–gel method. Briefly, $Ce(NO_3)_3 \cdot 6H_2O$ was mixed with a suitable amount of water–ethanol solution first. Then a small amount of dilute HNO_3 was added to the mixture. Citric acid and polyethylene glycol (molecular weight = 6000) were added as chelating agent and cross-linking agent, respectively. Highly transparent sols were obtained after being stirred for a few hours. The dopant Er^{3+} ions were introduced into the sol by adding $Er(NO_3)_3$ aqueous solution to the precursors solution. Then enough water was added to the solution to form gel. The dry gel, obtained by drying the gel at 80 °C for about 20 h, was heated at 400 °C for about 4 h, then grinded, and sintered at 700–900 °C for 1 h to get the CeO_2:Er^{3+} powders.

X-ray diffraction (XRD) was carried out on a MAC Science Co. Ltd. (Japan) MXP18AHF XRD apparatus with Cu$K\alpha$ radiation. The infrared spectra were recorded in the range 4000–400 cm^{-1} with a Magna-IR 750 FT-IR spectrometer.

The green and red upconversion emission were measured and analyzed by using a Jobin-Yvon LABRAM-HR confocal laser micro-Raman spectrometer system equipped with a semiconductor 785 nm laser (with a maximum power of 1 mW). All the measurements were carried out at room temperature.

3. Results and discussion

3.1. Structural properties

Fig. 1 gives the XRD patterns of CeO_2:Er^{3+} (1%) powders heat-treated at temperature 700–900 °C and the reference data of JCPDS Card no. 81-0792 for pure CeO_2.

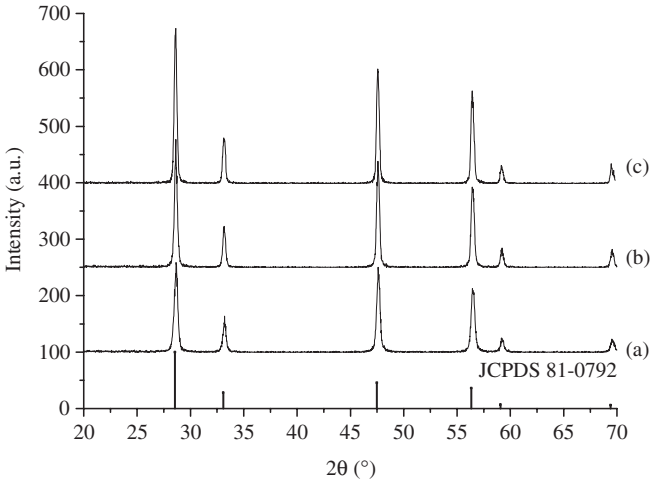

Fig. 1. Powder X-ray diffraction patterns of CeO_2:Er^{3+} (1%) powders heat-treated at (a) 700 °C, (b) 800 °C, (c) 900 °C for 1 h, and the reference data of JCPDS Card no. 81-0792 for pure CeO_2.

The diffraction patterns exhibit the samples crystallized in face-centered cubic fluorite (CaF_2) crystal structure ($a = 5.411$ Å). It can be seen that the intensity of diffraction peak increases and half width of diffraction peak decreases with annealing temperature, which indicates that the crystallite size of CeO_2 grain increases with the annealing temperature.

The upconversion efficiency is governed principally by the nonradiative processes of materials [5,11,13]. The multi-phonon nonradiative decay rate is given by the well-known energy gap law [11,25]:

$$W_n = W_0[1 - \exp(-h\nu/kT)]^{-n}, \quad (1)$$

where W_n is the rate at temperature T, W_0 the rate at 0 K, $n = \Delta E/h\nu$, ΔE is the energy gap between the levels involved, ν is the relevant phonon's frequency. When ΔE is equal to or less than 4–5 times the high-energy phonons, the multi-phonon nonradiative relaxation with the emission of a few high-energy phonons becomes competitive with the radiative processes.

Groups with high vibrational frequency in materials will increase the multi-phonon nonradiative rate and then will decrease the upconversion efficiency. The phonon cutoff of CeO_2 powders is quite low, but CO and OH groups that causing the high-energy vibrations may still exist in samples because of the limitation of sol–gel process.

FT-IR was used to investigate the organic residua in CeO_2 powders. Fig. 2 presents the FT-IR transmission spectra of CeO_2:Er^{3+} (1%) annealed at 700 °C (a), 800 °C (b) and 900 °C(c) in paraffin pellets and pure paraffin (d) as a reference. The band around 400–550 cm^{-1} is assigned to the Ce–O vibration of cubic CeO_2, which is in principle agreed with Ref. [22]. It should be stated that the phonon absorption edge does not appear to change significantly with annealing temperature, which is consistent with XRD patterns. It is clear that there are no absorption bands of OH groups (around 3400 cm^{-1}) and CO groups (around

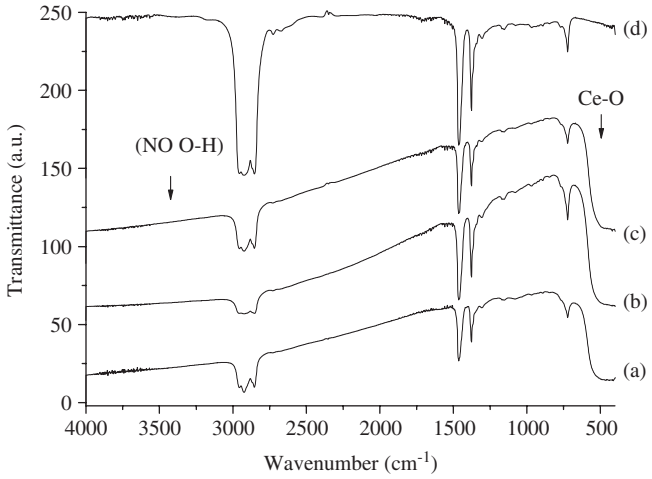

Fig. 2. FT-IR spectra of CeO_2:Er^{3+} (1%) heat-treated for 1 h at (a) 700 °C, (b) 800 °C, (c) 900 °C in paraffin pellets and pure paraffin (d) as a reference.

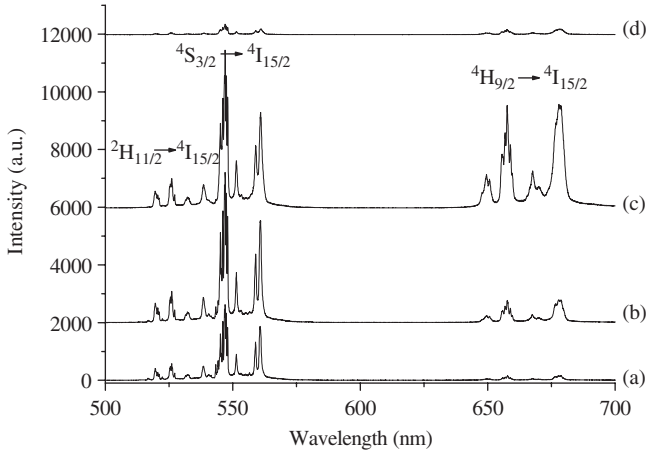

Fig. 3. Upconversion spectra of Er^{3+}-doped CeO_2 powders with different Er^{3+} concentration: (a) 0.5%, (b) 1%, (c) 3% and (d) 6% ($\lambda_{ex} = 785$ nm).

1500 cm^{-1}) in FT-IR spectra of all CeO_2:Er^{3+} samples, which implies that CeO_2:Er^{3+} samples may have higher upconversion luminescence efficiency.

3.2. Upconversion properties

Fig. 3 is the upconversion luminescence spectra of CeO_2:Er^{3+} powders with different doping concentration under 785 nm excitation. The sharp peaks in the green region 517–543 and 543–565 nm are assigned to the transition $^2H_{11/2} \rightarrow {}^4I_{15/2}$ and $^4S_{3/2} \rightarrow {}^4I_{15/2}$, respectively, while the peaks in the red region 645–682 nm are assigned to $^4F_{9/2} \rightarrow {}^4I_{15/2}$ transitions [10,11]. Fig. 3 indicates that when the doping concentration is lower than 3%, the emission intensities and the intensity ratio of red emission to that of green emission increase with Er^{3+} concentration. It also shows that the emission of CeO_2:Er^{3+} quenched at higher doping concentration (6%). The Er^{3+} ions in low concentration are usually randomly distributed in the host lattice and Er^{3+}–Er^{3+} distances are too far apart, but at higher concentration the distances between two Er^{3+} ions are reduced, thus leading to formation of Er^{3+} clusters. As a result, concentration-quenching processes will be the predominant nonradiative decay processes at higher concentration. In CeO_2:Er^{3+} powders, the quenching concentration (QC) is about 3%. Such a value is higher than that of TiO_2:Er^{3+} powders (QC = 0.5%) and $BaTiO_3$:Er^{3+} powders (QC = 0.25%) [15].

Fig. 4 gives the upconverted emission spectra of the 1% Er^{3+}-doped CeO_2 powders prepared at three different annealing temperatures. It is clear that the emission intensities increase with the annealing temperature. In this research, the samples have the same crystal phase (face-centered cubic structure) with different temperatures, but the particle size increases and the number of defects of the particles decreases with the increasing processing temperature. This indicates that the upconversion process is

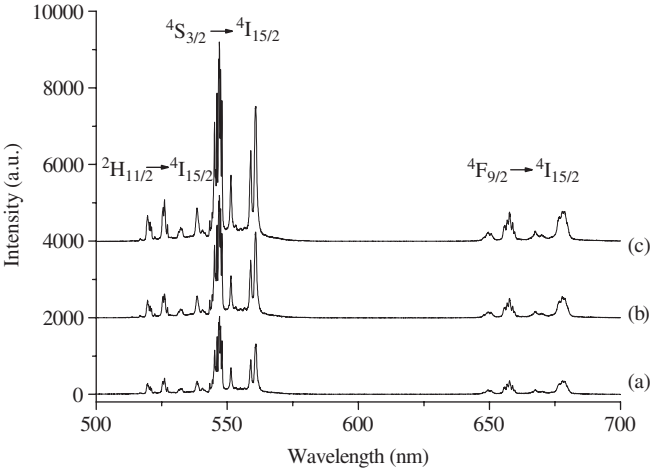

Fig. 4. Upconversion spectra of CeO_2:Er^{3+} (1%) powders heat-treated at (a) 700 °C, (b) 800 °C and (c) 900 °C for 1 h ($\lambda_{ex} = 785$ nm).

dependent not only on the Er^{3+} concentration but also on the annealing temperature.

In order to understand the energy upconversion mechanisms of the observed luminescent peaks, the upconverted luminescence intensity I of these transitions was measured as a function of pump power P. It is well known that I is proportional to the nth power of P, i.e.

$$I \propto P^n, \tag{2}$$

where n is the number of pump photons absorbed per upconverted photon emitted [10,11]. A plot of $\log I$ versus $\log P$ yield a straight line with slope n. The power dependence of I was shown in Figs. 5 and 6 for CeO_2:Er^{3+} (1%) and CeO_2:Er^{3+} (3%) samples, respectively. For CeO_2:Er^{3+} (1%) samples, the slope value n obtained were 1.80 ± 0.08, 1.74 ± 0.03 and 1.72 ± 0.02 for 526 nm ($^2H_{11/2} \rightarrow {}^4I_{15/2}$), 547 nm ($^4S_{3/2} \rightarrow {}^4I_{15/2}$) and 658 nm ($^4F_{9/2} \rightarrow {}^4I_{15/2}$)

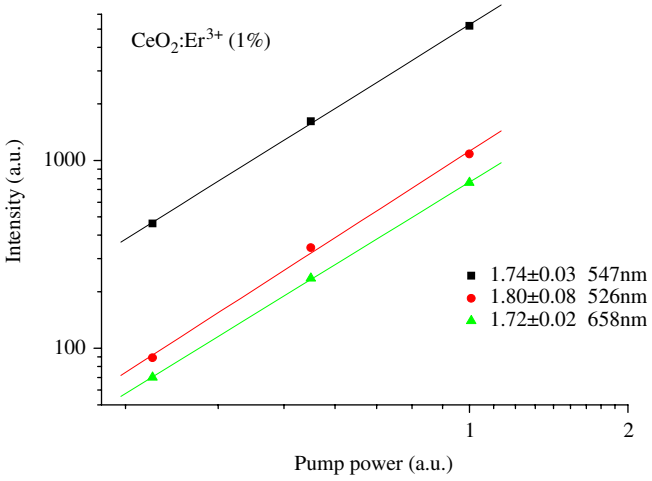

Fig. 5. Dependence of the upconversion emissions intensities on excitation power in CeO_2:Er^{3+} (1%) heat-treated at 900 °C.

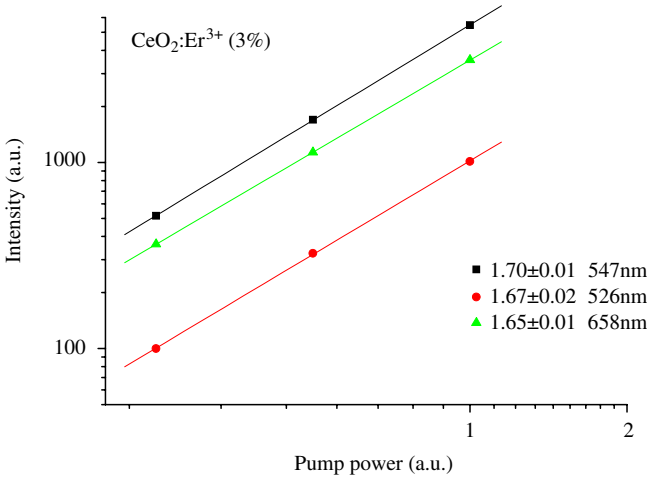

Fig. 6. Dependence of the upconversion emissions intensities on excitation power in CeO_2:Er^{3+} (3%) heat-treated at 900 °C.

emissions, respectively. For CeO_2:Er^{3+} (3%) samples (Fig. 6), the obtained n were 1.67 ± 0.02, 1.70 ± 0.01 and 1.65 ± 0.01 for 526 nm ($^2H_{11/2}\rightarrow{}^4I_{15/2}$), 547 nm ($^4S_{3/2}\rightarrow{}^4I_{15/2}$) and 658 nm ($^4F_{9/2}\rightarrow{}^4I_{15/2}$) emissions, respectively. These results show that two-photon process is responsible for green and red upconversion.

The excited states for upconversion can be populated by several well-known mechanisms: (1) ESA, (2) ET and (3) photon avalanche [4,5]. Photon avalanche was ruled out as a possible mechanism for upconversion because no inflection point was observed in the power study. Now, we will analyze the upconversion paths in CeO_2:Er^{3+}. Fig. 7 pictures energy level diagram of Er^{3+} ions as well as the probable upconversion mechanisms accounting for the green and red emissions under 785 nm excitation [10].

Er^{3+} ions are excited from the ground state to $^4I_{9/2}$ level by absorbing one 785 nm laser photon. From $^4I_{9/2}$ level, the Er^{3+} decays through a nonradiative process into $^4I_{11/2}$

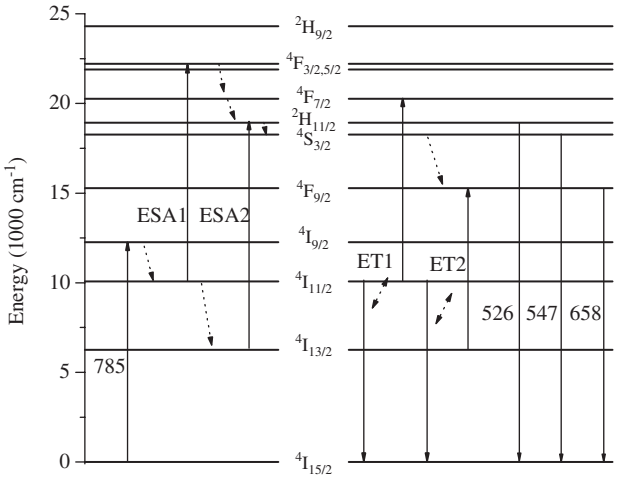

Fig. 7. Energy level diagrams of Er^{3+} ions in CeO_2 and upconversion mechanisms.

metastable level and subsequently into the $^4I_{13/2}$ metastable level. The ions in the $^4I_{11/2}$ level sequentially absorb another 785 nm photon and are raised to $^4F_{3/2,5/2}$ levels. This is an ESA process, labeled as ESA1 (in Fig. 7). The ions in the $^4F_{3/2,5/2}$ levels undergo multi-phonon relaxation through $^4F_{7/2}$ to $^2H_{11/2}$ and $^4S_{3/2}$ levels. Another possible ESA route, that can populate the $^4S_{3/2}$ level also, is the absorption of 785 nm photon from $^4I_{13/2}$ level to $^2H_{11/2}$ level (Fig. 7: ESA2). There is a possible ET route that can also populate those luminescent levels [11]. An excited ion relaxes from $^4I_{11/2}$ level to $^4I_{15/2}$ level nonradiatively and transfers the excitation energy to a neighboring ion in the same level, promoting the later to $^4F_{7/2}$ level:

$$^4I_{11/2}+{}^4I_{11/2}\rightarrow{}^4I_{15/2}+{}^4F_{7/2}(\text{Fig. 7 : ET1}).$$

The $^4F_{9/2}$ level can be possibly pumped via a nonradiative relaxation from the $^4S_{3/2}$ excited state with a moderate rate. The rate is given by Eq. (1). Due to the low phonon cutoff of CeO_2 host and the energy gap ΔE between $^4S_{3/2}$ and $^4F_{9/2}$ levels is about 3200 cm^{-1}, it requires at least 6 phonons to bridge this energy gap. As a result, the nonradiative relaxation from $^4S_{3/2}$ level is inefficient, which is confirmed by the low intensity of red emissions in low doping concentration samples (Figs. 3a and b and 4). From the different intensities ratio of red emissions versus green emissions in different Er^{3+} ions concentration samples (in Fig. 3), it is reasonable to assume that there must be another ET process that only populates the $^4F_{9/2}$ level. This ET process can be described as

$$^4I_{13/2}+{}^4I_{11/2}\rightarrow{}^4F_{9/2}+{}^4I_{15/2}(\text{Fig. 7 : ET2}).$$

The populated $^4I_{13/2}$ level may be excited through multi-phonon nonradiative process from $^4I_{11/2}$ level and radiative process from upper levels, such as $^4S_{3/2}$ level.

The enhancement of the red emissions with respect to the green emissions indicates that ET1 and ET2 processes do not depend in the same way on the Er^{3+} ions concentration. In fact, ET2 process is more effective than ET1

process as a function of increasing concentrations. This may be due to the fact that the ET processes involved in the two mechanisms are of different nature (i.e., dipole–dipole, dipole–quadrupole, etc.) [2].

ESA process is a single-ion process and is independent of the ions concentration, while ET process involves two ions and ET process rate will increase with Er^{3+} ions concentration. Usually, for low concentration samples (CeO_2:Er^{3+} (0.5%) and CeO_2:Er^{3+} (1%)), ESA1 and ESA2 processes are the dominant excitation routes for green emissions, and nonradiative relaxation from the $^4S_{3/2}$ level is the dominant mechanism for red emissions. While for high concentration samples (CeO_2:Er^{3+} (3%)), ESA1, ESA2 and ET1 processes are the dominant excitation routes for green emissions, and ET2 process is the dominant mechanism for red emissions.

4. Conclusions

CeO_2:Er^{3+} powders were prepared by Pechini type sol–gel method. XRD patterns show that the samples crystallized in typical cubic CeO_2 structure. FT-IR spectra show that CeO_2 powders sintered at 900 °C may present higher upconversion efficiency because of its low vibrational frequency.

Under 785 nm laser excitation, the samples show strong green and red upconversion emissions. Spectra show that the QC of upconversion is about 3% and the emission intensities increase with the annealing temperature. The laser power dependence on upconverted emissions revealed that two-photon process lead to green and red emissions. The upconversion mechanisms are ascribed as ESA process from $^4I_{11/2}$ level to $^4F_{3/2,5/2}$ levels, from $^4I_{13/2}$ level to $^2H_{11/2}$ level and ET process: $^4I_{11/2}+{}^4I_{11/2}\rightarrow{}^4I_{15/2}+{}^4F_{7/2}$, $^4I_{13/2}+{}^4I_{11/2}\rightarrow{}^4F_{9/2}+{}^4I_{15/2}$. The upconversion properties indicate that CeO_2:Er^{3+} may be used in upconversion phosphors.

References

[1] F. Heine, E. Heumann, T. Danger, T. Schweizer, G. Huber, B. Chai, Appl. Phys. Lett. 65 (1994) 383.
[2] X. Chen, T. Nguyen, Q. Luu, B. Di Bartolo, J. Lumin. 85 (2000) 295.
[3] J. Li, J. Wang, H. Tan, X. Cheng, F. Song, H. Zhang, S. Zhao, J. Cryst. Growth 256 (2003) 324.
[4] F. Vetrone, J.C. Boyer, J.A. Capobianco, A. Speghini, M. Bettinelli, Chem. Mater. 15 (2003) 2737.
[5] F. Vetrone, J.C. Boyer, J.A. Capobianco, A. Speghini, M. Bettinelli, J. Phys. Chem. B 106 (2002) 5622.
[6] F. Vetrone, J.C. Boyer, J.A. Capobianco, A. Speghini, M. Bettinelli, J. Phys. Chem. B 107 (2003) 1107.
[7] J.A. Capobianco, F. Vetrone, J.C. Boyer, A. Speghini, M. Bettinelli, J. Phys. Chem. B 106 (2002) 1181.
[8] D. Matsuura, Appl. Phys. Lett. 81 (2002) 4526.
[9] D. Dosev, I.M. Kennedy, M. Godlewski, I. Gryczynski, K. Tomsia, E.M. Goldys, Appl. Phys. Lett. 88 (2006).
[10] H. Lin, G. Meredith, S. Jiang, X. Peng, T. Luo, N. Peyghambarian, E. Yue-Bun Pun, J. Appl. Phys. 93 (2003) 186.
[11] H. Guo, N. Dong, M. Yin, W. Zhang, L. Lou, S. Xia, J. Phys. Chem. B 108 (2004) 19205.
[12] H. Guo, Y. Li, D. Wang, W. Zhang, M. Yin, L. Lou, S. Xia, J. Alloy Compd. 376 (2004) 23.
[13] A. Patra, C.S. Friend, R. Kapoor, P.N. Prasad, Appl. Phys. Lett. 83 (2003) 284.
[14] A. Patra, P. Ghosh, P.S. Chowdhury, M.A.R.C. Alencar, L.B. Whualkuer, N. Rakov, G.S. Maciel, J. Phys. Chem. B 109 (2005) 10142.
[15] A. Patra, C.S. Friend, R. Kapoor, P.N. Prasad, Chem. Mater. 15 (2003) 3650.
[16] H. Guo, N. Dong, M. Yin, W. Zhang, L. Lou, S. Xia, J. Alloy Compd. 415 (2006) 280.
[17] M. Pang, J. Lin, J. Cryst. rowth 284 (2005) 262.
[18] S. Heer, K. Kompe, H.U. Gudel, M. Haase, Adv. Mater. 16 (2004) 2102.
[19] S. Heer, O. Lehmann, M. Haase, H.U. Gudel, Angew. Chem.—Int. Ed. 42 (2003) 3179.
[20] F. van de Rijke, H. Zijlmans, S. Li, T. Vail, A.K. Raap, R.S. Niedbala, H.J. Tanke, Nat. Biotechnol. 19 (2001) 273.
[21] F. Auzel, Chem. Rev. 104 (2004) 139.
[22] C. Ho, J.C. Yu, T. Kwong, A.C. Mak, S. Lai, Chem. Mater. 17 (2005) 4514.
[23] S. Wang, W. Wang, J. Zuo, Y. Qian, Mater. Chem. Phys. 68 (2001) 246.
[24] W.H. Weber, K.C. Hass, J.R. McBride, Phys. Rev. B 48 (1993) 178.
[25] G. Blasse, B.C. Grabmaier, Luminescent Materials, Springer, Berlin, 1994.